Nylon 6 Crystal-Phase Transition in Nylon 6/Clay/ Poly(vinyl alcohol) Nanocomposites

Li Cui,[1] Jen-Taut Yeh[1,2,3]

[1]*Key Laboratory of Green Processing and Function Textiles of New Textile Materials (Ministry of Education), Wuhan University of Science and Engineering, Wuhan, China*
[2]*Faculty of Material Science and Engineering, Hubei University, Wuhan, China*
[3]*Department of Polymer Engineering, National Taiwan University of Science and Technology, Taipei, Taiwan*

Received 13 January 2010; accepted 7 April 2010
DOI 10.1002/app.32578
Published online 3 June 2010 in Wiley InterScience (www.interscience.wiley.com).

ABSTRACT: A study of the dependence of the poly(vinyl alcohol) (PVA) content on the nylon 6 crystal-phase transition properties and PVA morphologies of nylon 6/clay nanocomposite (NYC)/PVA specimens was conducted. The degree of compatibility between NYC and PVA was examined by dynamic mechanical analysis measurement. The strong hydrogen bonding between the nylon 6 and PVA molecules led to nearly complete inhibition of PVA crystallization when the PVA contents were less than 16.7 wt %. Moreover, scanning electron microscopy analysis indicated that the clays originally present in the nylon 6 matrices migrated gradually into the PVA phases with increasing PVA content in the NYC/PVA series specimens. This interesting migration of clay from nylon 6 to PVA led to a nylon 6 crystal-phase transition from the γ to the α form. © 2010 Wiley Periodicals, Inc. J Appl Polym Sci 118: 1683–1690, 2010

Key words: blends; nylon; organoclay

INTRODUCTION

Nylon 6 is a highly crystalline polymer with two crystalline phases, α and γ forms.[1–5] The α form is composed of a fully extended planar zigzag chain conformation, in which adjacent antiparallel chains are joined to each other by hydrogen bonds. It is the most thermodynamically stable crystalline form and can be obtained by slow cooling from the melt. The γ form consists of pleated sheets of parallel chains joined by hydrogen bonds; it is less stable and can be obtained by fast cooling from the melt or fiber spinning at a high speed.[6,7] It was reported[8] that the γ-form nylon 6 crystals can be converted into the α form by recrystallization from the melt, the application of stress at room temperature, or annealing of the γ-form nylon 6 crystals at 160°C in a saturated steam atmosphere.

The modification of the barrier and physical properties of polymers with nanoscale filler particles with a high surface area to thickness aspect ratio has drawn much attention recently,[9,10] wherein the filler particles (e.g., smectite clays) are typically approximately 1 nm thick with lateral dimensions on the order of 200–1000 nm. Significant improvements in the modulus and heat deflection temperature were first found in nylon 6/clay nanocomposites (NYCs) with the addition of 2–8 wt % smectite clays.[11,12] Later, investigators found that the clay platelets had a noticeable nucleating effect on the formation of γ-form nylon 6 crystals in NYCs.[11–16] As suggested by several investigators,[17–19] protonated amino end groups of the nylon 6 molecules can be ionically bonded to the surfaces of negatively charged silicate sheets, which then leads to a poorly arranged nylon 6 conformation gathered on the surfaces of the silicate sheets. These poorly arranged nylon 6 molecules then serve as the nucleation sites and, hence, cause the formation of γ-form nylon 6 crystals during the crystallization processes of NYC melts, although the α-form crystals with nylon 6 molecules linearly aligned in the unit cells are the more stable form.

Poly(vinyl alcohol) (PVA) is well known for its low cost, excellent transparency, flexibility, toughness, biodegradability, and gas barrier properties and, hence, is widely used in textile sizing and/or as a finishing agent, emulsifier, photosensitive coating, food package, and/or adhesive for paper, wood, textiles, and leather.[20–22] However, PVA can seldom be used as a thermoplastic polymer because of its high water absorption and weak thermal stability. Ha and Lee[23] reported that the formation of the α-crystal forms of nylon 6 molecules was nearly not affected by the blending of various amounts of poly(vinyl acetate), hydroxylated PVA, or PVA in nylon 6 resin. However, as far as we know, hardly any investigation have been reported on the melt blending and

Correspondence to: L. Cui (18635923@qq.com).

crystal-form transformation of nylon 6 molecules in NYC/PVA nanocomposites.

The main objective of this study was to investigate the crystalline-form transformation properties of nylon 6 molecules in NYC/PVA nanocomposites. After the addition of PVA to NYC resins, the major γ-form nylon 6 crystals originally present in NYC resins were found to transform into α-form crystals with increasing PVA content. In fact, almost only α-form nylon 6 crystals were found in the NYC/PVA nanocomposites with PVA contents of 50 wt % or greater. To understand these interesting γ-to-α crystal-phase transition properties of nylon 6 molecules in the NYC/PVA nanocomposites, thermal, X-ray diffraction analysis of NYC/PVA specimens and/or scanning electron microscopy (SEM) analysis of the chemically and physically etched NYC/PVA specimens were carried out. Possible reasons for the interesting crystalline-phase transition properties of the nylon 6 molecules in the NYC/PVA nanocomposites are proposed.

EXPERIMENTAL

Materials and sample preparation

PVA was obtained from Oriental Chemical Industries (Seoul, Korea) in granule form with the trade name Polinol F26 [degree of polymerization = 2600, hydrolysis (dry basis) = 98–99 mol %]. The nylon 6/clay (NYC) nanocomposite used in this study was obtained from Unitika, Ltd. (Tokyo, Japan) with the trade name M1030D. The M1030D nylon 6/clay resin was cited with a weight-average molecular weight of 62,000 and 4.6 wt % exfoliated montmorillonite.

The NYC/PVA specimens were prepared by melt blending with a SU-70 Plasti-Corder Mixer, which was purchased from Suyuan Science and Technology Corp. (Chang Zhou, China). Before melt blending, the NYC and PVA resins were dried in a vacuum oven at 80°C for 12, 12, and 8 h, respectively. The dried components of NYC/PVA at various weight ratios were then melt-blended in the Plasti-Corder Mixer. During each melt-blending process, the Plasti-Corder Mixer was operated at 240°C with a screw speed of 250 rpm for 4 min. The compositions of the NYC/PVA series specimens prepared in this study are summarized in Table I.

TABLE I
Compositions of the NYC/PVA Specimens

Specimen	NYC (%)	PVA (%)
NYC	100	0
NYC_7PVA_1	87.5	12.5
NYC_5PVA_1	83.3	16.7
NYC_3PVA_1	75.0	25.0
NYC_1PVA_1	50.0	50.0
NYC_1PVA_3	25.0	75.0
PVA	0	100

Dynamic mechanical analysis (DMA)

DMA was carried out with a TA Instruments Q800 DMA instrument (New Castle, DE). All of the NYC/PVA samples were measured in tensile mode over the temperature range −40 to 150°C at a heating rate of 3°C/min and with a frequency of 1 Hz. The specimen dimensions were 60 × 4 × 0.3 mm^3.

Thermal properties

The thermal properties of the NYC, PVA, and NYC/PVA series resins were determined at 25°C with a TA Q100 differential scanning calorimetry (DSC) instrument. All scans were carried out at a heating rate of 20°C/min and under flowing nitrogen with a flow rate of 50 mL/min. The instrument was calibrated with pure indium. Samples weighing about 0.5 mg were placed in standard aluminum sample pans for each DSC experiment. The percentage crystallinity (X_c) values of the γ and α forms of the nylon 6 crystals in the NYC/PVA specimens were estimated with an origin peak fitting module to divide the overlapped melt endotherm. The perfect heat of fusions (ΔH_m^0's) of the γ and α forms of the nylon 6 crystals were 239 and 241 J/g,[23] respectively. The X_c values were evaluated as follows:

$$X_c(\%) = \frac{A\% \times \Delta H_m}{\Delta H_m^0} \times 100\%$$

where A% is the melt endotherm area percentage of the γ or α form of the nylon 6 crystals in the overlapped peak and ΔH_m is the melting enthalpy of crystallization of nylon 6 in the NYC/PVA specimens.

Wide-angle X-ray diffraction (WAXD)

The WAXD properties of the NYC, PVA, and NYC/PVA specimens were determined with a Siemens D5000D diffractometer equipped with Ni-filtered Cu Kα radiation operated at 35 kV and 25 mA (Munich, Germany). Each specimen was 1 mm thick and was maintained stationary at 25°C and scanned in the reflection mode from 2 to 40° at a scanning rate of 5°/min.

Morphology of the NYC/PVA specimens

To determine the morphology of the NYC/PVA specimens, the samples were fractured in liquid nitrogen and then etched with physical etching

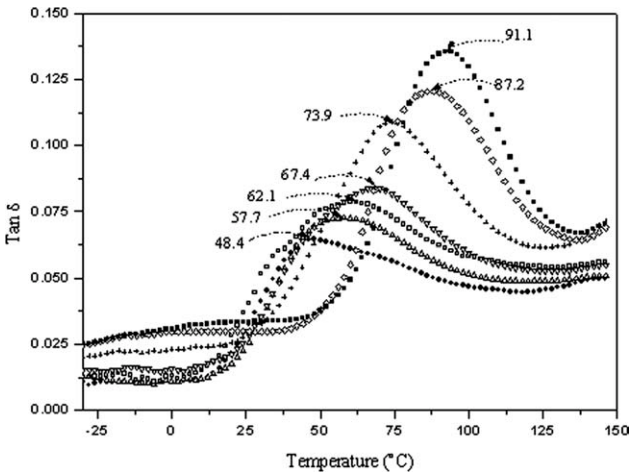

Figure 1 Temperature dependence of tan δ at 1 Hz for (●) NYC, (△) NYC_7PVA_1, (□) NYC_5PVA_1, (▽) NYC_3PVA_1, (+) NYC_1PVA_1, (◇) NYC_1PVA_3, and (■) PVA specimens.

methods. The physical etching was used to make contrasts among nylon6, PVA, and the clay. The fractured surface of the specimen was subject to argon-ion bombardment at 2000 eV for 3 min during the physical etching treatment. The beam was focused perpendicularly to the surface of the specimens. Depending on the different resistances of the components to the ion-beam etching (Clay > Nylon 6 > PVA), the phase morphology and the location of the clay in the blend could be studied by this method. The etched samples were then gold-coated and examined by an X-650 Hitachi scanning electron microscope at 20 kV (Tokyo, Japan).

RESULTS AND DISCUSSION

DMA

The temperature dependences of the tan δ of the NYC, NYC/PVA, and PVA specimens and the corresponding peak values are summarized in Figure 1. Only one tan δ transition, with a peak temperature ranging from 48.4 to 91.1°C, was observed in the tan δ plot of each NYC, PVA, and NYC/PVA specimen. The tan δ peak temperatures of the NYC and PVA specimens were at 48.4 and 91.1°C, respectively. In fact, the peak temperatures of the tan δ transitions of the NYC/PVA specimens increased consistently as their PVA contents increased. For instance, the glass-transition temperatures (T_g's) of the NYC/PVA specimens increased from 57.7 to 73.9°C as their PVA contents increased from 12.5 to 50 wt %. The tan δ transitions observed for the NYC, PVA, and NYC/PVA specimens were most likely due to their corresponding glass transitions, which were associated with the relaxation of the main backbone chains in the amorphous phases. The single tan δ transitions observed for the NYC/PVA specimens prepared in this study suggested that the nylon 6 molecules were miscible with those PVA molecules present in the amorphous phases at a limited degree because the tan δ transitions for NYC and PVA were very close. Presumably, the reasons that the T_g of NYC used in our research was significantly lower than that of the typical one were as follows: (1) a little water still in the specimen that could not be removed by drying in a vacuum oven at 80°C for 12 h, (2) the structure of the molecular chain, and (3) the degradation of NYC in the second heat processing at 240°C.

Thermal properties

Typical DSC thermograms of the NYC, PVA, and NYC/PVA series specimens are shown in Figure 2. The DSC thermogram of the NYC specimen showed a double melting endotherm with a main melting peak temperature around 214°C. Another minor melting endotherm with a higher peak temperature around 220°C was found on the right shoulder of the main melting endotherm of the NYC specimen. Only one main melting endotherm was found on the DSC thermogram of the PVA resin, in which the melting temperature of the PVA resin was at 230.9°C. In contrast, after PVA was blended in NYC, the characteristics of most DSC thermograms of the NYC/PVA specimens were similar to the combination of those of the NYC and PVA specimens. However, the sizes associated with the main melting endotherms of NYC and PVA decreased significantly with increasing PVA and NYC contents of the NYC/PVA specimens, respectively. On the other hand, the melting endotherm of PVA present in the

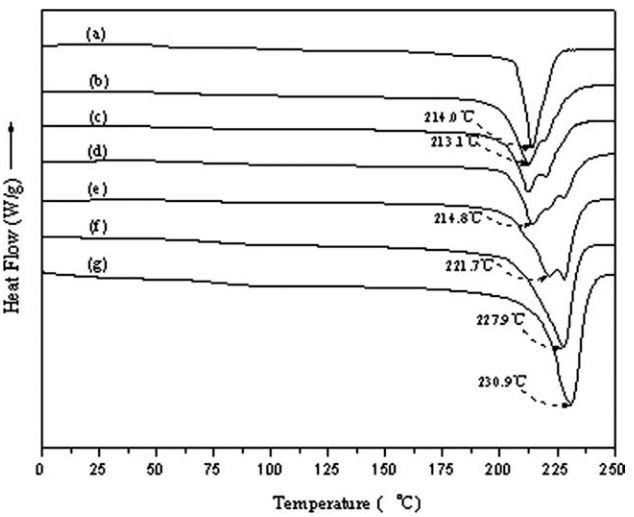

Figure 2 DSC thermograms of (a) NYC, (b) NYC_7PVA_1, (c) NYC_5PVA_1, (d) NYC_3 PVA_1, (e) NYC_1PVA_1, (f) NYC_1PVA_3, and (g) PVA specimens.

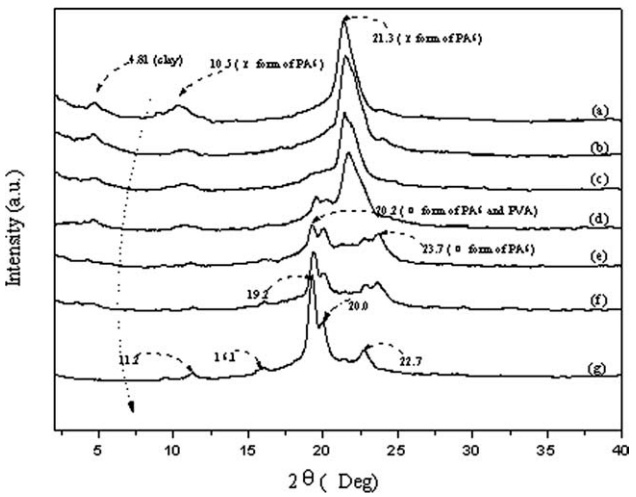

Figure 3 Wide-angle X-ray scattering diffraction patterns of (a) NYC, (b) NYC_7PVA_1, (c) NYC_5PVA_1, (d) NYC_3PVA_1, (e) NYC_1PVA_1, (f) NYC_1PVA_3, and (g) PVA specimens (PA6 refers to nylon 6 in NYC).

NYC/PVA specimens disappeared quickly as their NYC content increased. Almost no PVA melting endotherm could be found on the DSC thermograms of the NYC/PVA specimens when the PVA content was less than 16.7 wt % [see Fig. 2(b)]. Interestingly, the size of the minor but higher melting endotherm of the NYC resin grew at the expense of the main but lower melting endotherm as the PVA content of the NYC/PVA specimens increased. In fact, the lower melting endotherm originally shown on the double melting endotherm of the NYC resin could barely be seen when the weight ratios of PVA to NYC of the NYC/PVA specimens were equal to or greater than 1 (i.e., the NYC_1PVA_1 and NYC_1PVA_3 samples).

WAXD

Typical X-ray diffraction patterns and peak diffraction angles of the NYC, PVA, and NYC/PVA series specimens are shown in Figure 3. The crystals of the PVA specimen crystallized at 25°C were α-form crystals, which corresponded to peak X-ray diffraction angles at 11.2, 16.1, 19.2, 20.0, and 22.7°.[15] Similar to the results found in our previous investigations,[24] the crystals of the NYC specimen crystallized at 25°C were γ-form crystals, which corresponded to a peak X-ray diffraction angle at 21.3°.[25] After the PVA was blended in the NYC resins, the characteristics of the X-ray diffraction patterns of the NYC/PVA specimens were very similar to those of the NYC and PVA specimens, wherein γ-form nylon 6 crystals and α-form PVA crystals were the main crystals present in the NYC/PVA specimens, although the diffraction patterns of the α-form PVA crystal could barely be found because their weight ratios of PVA to NYC of the NYC/PVA specimens were less than 1 : 5 (i.e., the NYC_5PVA_1 and NYC_7PVA_1 samples). In contrast, α-form nylon crystals with peak diffraction angles at 20.3 and 23.7° started to grow at the expense of γ-form nylon 6 crystals as the PVA contents of the NYC/PVA specimens increased (see Fig. 3). In fact, γ-form nylon 6 crystals originally present in the NYC resin almost disappeared when the weight ratios of PVA to NYC of the NYC/PVA specimens were equal to or greater than 1 (i.e., the NYC_1PVA_1 and NYC_1PVA_3 specimens). Compared with the WAXD analysis, the size of the minor but higher melting endotherm of the NYC resin grew at the expense of the main but lower melting endotherm when the PVA content of the NYC/PVA specimens increased. The γ form, which consisted of pleated sheets of parallel chains joined by hydrogen bonds, always exhibited lower melting points than the α-crystal form, which had a two-dimensional arrangement. Therefore, the higher and lower melting endotherm peaks of the NYC resin observed in the DSC analysis were attributed to the α and γ forms of the nylon 6 crystals, respectively. As shown in Table II, the crystallinity of the α-form nylon 6 crystals increased significantly with increasing PVA content. Conversely, the crystallinity of the γ-form nylon 6 crystals originally existing in NYC decreased significantly and almost disappeared finally. Heating in DSC may have had an effect on the phase morphology and melting behavior of the blend. Probably, the heating process led to the crystal transition, but this was not the important factor because the phase transition was also observed in wide-angle X-ray scattering, which did not have a heating process.

On the other hand, the peak X-ray diffraction angle at 4.81° of the NYC specimen displayed X-ray diffraction from the (001) crystal surface of the clay layers present in the NYC resin,[26] which corresponded to a 1.84 nm *d*-spacing of the clay layers. In fact, the peak diffraction angles of the clay layers decreased significantly as the weight ratios of PVA to NYC increased; this indicated an increasing *d*-spacing of the clay layers of the NYC/PVA specimens (see Fig. 4). Apparently, the slightly aggregated clay layers present in the NYC specimen could be further dispersed by the mixture of PVA in the NYC specimen and, hence, caused an

TABLE II
Crystallinity of the γ and α Forms of the Nylon 6 Crystals in the NYC/PVA Specimens

	X_c (%)	
Specimen	γ form	α form
NYC	27.1	2.1
NYC_7PVA_1	25.7	2.3
NYC_5PVA_1	20.6	4.5
NYC_3PVA_1	16.4	8.3
NYC_1PVA_1	2.3	21.7
NYC_1PVA_3	2.0	20.4

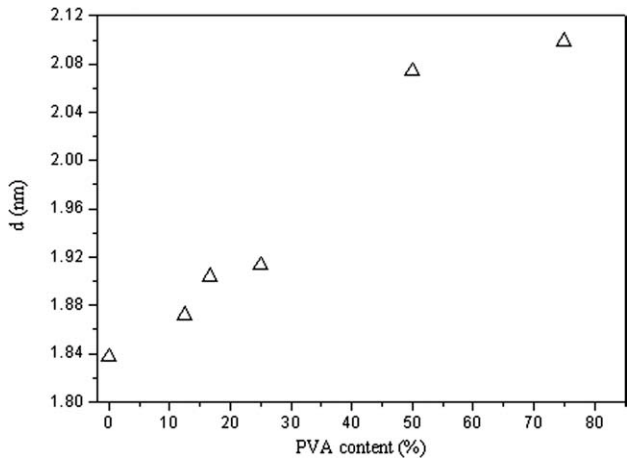

Figure 4 Evaluated *d*-spacing values of clay layers present in the NYC/PVA specimens.

increase in the *d*-spacing of the clay layers as the weight ratios of PVA to NYC in the NYC/PVA specimens increased. For instance, the *d*-spacing values of the clay layers increased significantly from 1.83 to 2.10 nm in the NYC/PVA specimens as their PVA contents increased from 0 to 75 wt %. The increasing *d*-spacing of the clay layers was attributed to the fact that the shear force in the second processing increased as the viscosity of the melt blends increased with the addition of PVA to NYC, and the content of the clay in the sample decreased as the PVA content increased.

Morphological properties

Figure 5 summarizes SEM micrographs of the NYC and NYC/PVA series specimens etched after emission by ion beams. The sizes of the dispersed PVA

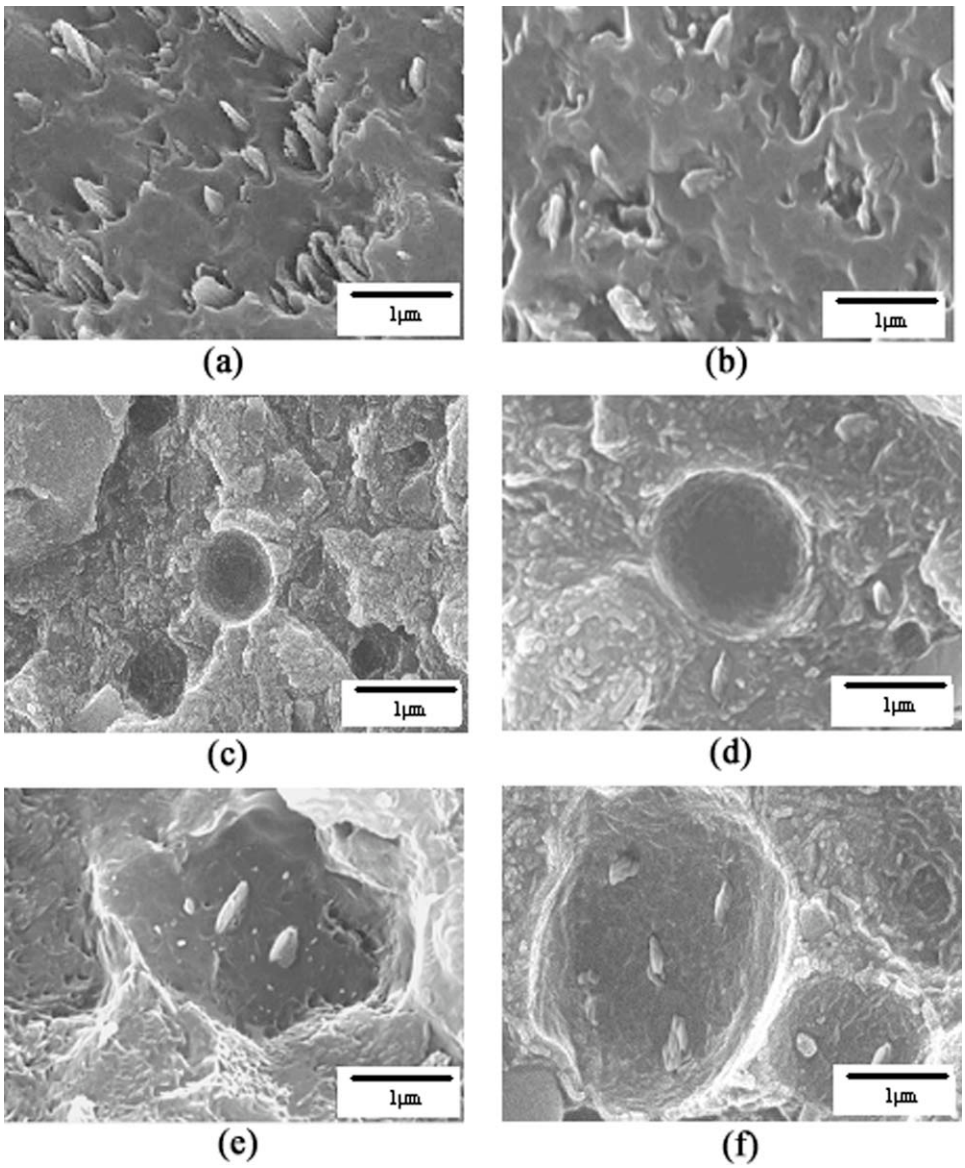

Figure 5 SEM micrographs of (a) NYC, (b) NYC_7PVA_1, (c) NYC_5PVA_1, (d) NYC_3PVA_1, (e) NYC_1PVA_1, and (f) NYC_1PVA_3 specimens etched by ion beams.

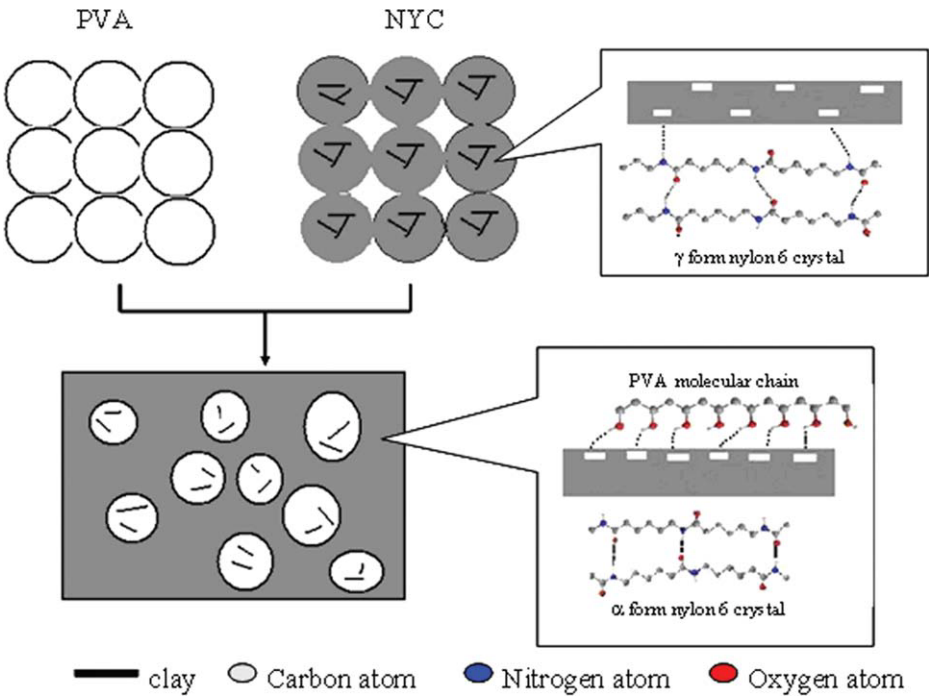

Figure 6 Sketch of the crystal-phase transition of nylon 6 in the NYCPVA specimens. [Color figure can be viewed in the online issue, which is available at www.interscience.wiley.com.]

phases, shown as the dark spots, on the etched surfaces of the NYC/PVA series specimens increased significantly with increasing PVA contents. At PVA contents less than 16.7 wt %, the morphology of the NYC/PVA series specimens were very similar to that of the based NYC specimen, in which only irregularly etched nylon 6 spots, rather than demarcated circular etched PVA dark spots, could be found on the etched surfaces of the NYC_7PVA_1 and NYC specimens [see Figure 5(a,b)]. As reported in the DSC and WAXD analysis, the characteristic melting endotherm and X-ray diffraction patterns corresponding to PVA crystals could barely be found when the PVA contents were lower than 16.7 wt %. On the basis of these results, we could reasonably infer that the disappearance of the dispersed PVA phases and PVA crystal characteristics at PVA contents lower than 16.7 wt % were most likely due to the inhibition of its crystallization because most of the PVA molecules were miscible and interacted strongly with the nylon 6 molecules by hydrogen bonding[16] in the amorphous and melt phases at PVA contents lower than 16.7 wt %. In fact, as evidenced by DMA, nylon 6 molecules had a degree of compatibility with those PVA molecules in the amorphous phases at PVA contents ranging from 12.5 to 75.0 wt %. As a result, the PVA crystal characteristics and dispersed PVA phases originally present in the NYC/PVA specimens disappeared nearly completely when the PVA contents were lower than 16.7 wt %. There may have been a possible phase inversion at greater contents of PVA. However, when the PVA content was equal to or less than 75 wt %, the phase inversion did not happen; presumably, it was mainly due to the fact that the viscosity of nylon 6 was significantly lower than that of PVA. Moreover, the clay in this blend may have locked its unstable morphology.[24]

On the other hand, interestingly, the clay remnants originally present in the etched PVA dark spots of the NYC/PVA series specimens were found to gradual transfer into the nylon 6 rich matrices when their PVA contents were lower than 50 wt % [see Fig. 5(a–d)]. In fact, the clay remnants could only be found in the etched nylon 6 rich matrices of the NYC/PVA specimens when their PVA contents were equal to or less than 16.7 wt % [see Fig. 5(a,b)]. These interesting morphological properties suggest that the clays originally present in the nylon 6 matrices migrated significantly into the PVA phases when the PVA contents blended into the NYC/PVA series specimens were equal to or greater than 50 wt %. Presumably, the dependence of the PVA content on the crystal-phase transition properties of the NYC/PVA specimens observed in the DSC and WAXD analysis could be attributed to the interesting clay migration behavior observed previously. As suggested by several investigators,[11–15] the protonated amino end groups of nylon 6 molecules can be ionically bonded to the surfaces of negatively charged silicate sheets, which then leads to a poorly arranged nylon 6 conformation gathered on the surfaces of the

silicate sheets. These poorly arranged nylon 6 molecules, therefore, served as nucleation sites and, hence, caused the formation of γ-form nylon 6 crystals during the crystallization processes of the NYC melts. However, fewer poorly arranged nylon 6 molecules were expected to gather on the surfaces of the silicate sheets, as the clays migrated gradually into the PVA phases as the PVA contents blended in the NYC/PVA specimens increased. Under such circumstances, the γ-form nylon 6 crystals originally present in the NYC specimen gradually transformed into α-form nylon 6 crystals as the PVA contents of the NYC/PVA specimens increased. It was, therefore, reasonable to believe that almost only α-form nylon 6 crystals could be found in the NYC/PVA specimens with PVA contents equal to or greater than 50 wt % because the clays were barely present in the nylon 6 rich phases but were mostly present in the separated PVA phases. Figure 6 is a sketch of the crystalline-phase transition of nylon 6 in the NYC/PVA specimens. Presumably, the interaction between PVA and clay was larger than that between nylon and clay because the polarity of —OH was significantly larger than that of amide groups. Under the conditions of melting temperature and high shear force, the nylon 6 and PVA molecular chains competed to attack clay. Moreover, the crystallization temperature of PVA was higher than that of nylon 6. So once the PVA molecular chain bonded on the clay surface, the nylon molecules were squeeze away during the PVA crystallization process. Because the nylon 6 molecules had a degree of compatibility with the PVA molecules in the amorphous phases and the PVA crystal characteristics were inhibited by the strong hydrogen bonding between PVA and the nylon 6 molecules, no separated PVA phases were observed when the PVA contents were less than 16.7 wt %. So, no clay immigration was observed. When the PVA contents were between 16.7 and 50 wt %, clay migration might have happened. However, the small clay migration from nylon 6 to the PVA phase slightly affected the crystal phase of nylon 6 or was overlapped by other obvious phenomena (see Table II). However, the migration of clay from nylon 6 into PVA was obvious when the PVA contents were greater than 50 wt %.

CONCLUSIONS

The characteristics of the melting endotherm and X-ray diffraction patterns of α-form PVA crystals nearly disappeared after less than 16.7 wt % PVA was blended in NYC resins. In contrast, the α-form nylon 6 crystals gradually grew at the expense of the γ-form nylon 6 crystals as the PVA contents of the NYC/PVA specimens increased, and the characteristics of the γ-form nylon 6 crystals originally shown on the melting endotherm and X-ray diffraction patterns of the NYC resin were barely seen when the PVA contents of the NYC/PVA specimens were equal to or greater than 50 wt %. Further SEM analysis of the NYC/PVA specimens indicated that the clay remnants were only found in the etched nylon 6 rich matrices of the NYC/PVA specimens when their PVA contents were less than 16.7 wt %. However, the clays originally present in the nylon 6 matrices migrated gradually into the PVA phases when the PVA contents of the NYC/PVA series specimens were equal to or greater than 50 wt %. The dependence of the PVA content on the crystal-phase transition properties of the NYC/PVA specimens were attributed to the interesting clay migration behavior.

As evidenced by DMA, nylon 6 molecules had a degree of compatibility with those PVA molecules in the amorphous phases at PVA contents ranging from 12.5 to 75.0 wt % because only a single tan δ transition was observed for those NYC/PVA specimens. However, many dispersed PVA phases were found on the surfaces of the NYC/PVA specimens etched by water or ion-beam emission, whereas the sizes of the dispersed PVA phases increased consistently as the PVA contents increased. However, the dispersed PVA phase original present in the NYC/PVA specimens disappeared nearly completely when their PVA contents were less than 16.7 wt %. Presumably, the disappearance of the dispersed PVA phases were attributed to the strong hydrogen bonding between the nylon 6 and PVA molecules; this led to nearly complete inhibition of PVA crystallization when the PVA contents were less than 16.7 wt %.

References

1. Miyasaka, K.; Ishikawa, K. J Polym Sci Part A-2: Polym Phys 1968, 6, 1317.
2. Miyasaka, K.; Ishikawa, K. J Polym Sci Part A-2: Polym Phys 1972, 10, 1497.
3. Kyotani, M. J Macromol Sci Phys 1975, 11, 509.
4. Murthy, N. S. Polym Commun 1991, 32, 301.
5. Ho, J.; Wei, K. Macromolecules 2000, 33, 5181.
6. Brucato, V.; Crippa, G.; Piccarolo, S.; Titomanlio, G. Polym Eng Sci 1991, 31, 1411.
7. Samon, J. M.; Schultz, J. M.; Wu, J.; Hsiao, B.; Yeh, H.; Kolb, R. J Polym Sci Part B: Polym Phys 1999, 37, 1277.
8. Murthy, N. S.; Szollosi, A. B.; Sibilia, J. P.; Krimm, S. J Polym Sci Polym Phys Ed 1985, 23, 2369.
9. Usuki, A.; Koiwai, A.; Kojima, Y.; Kawasumi, M.; Okada, A.; Kurauch, T.; Kamigaito, O. J Appl Polym Sci 1995, 55, 119.
10. Okada, A.; Fukushima, Y.; Kawasumi, M.; Inagaki, S.; Usuki, A.; Sugiyama, S.; Kurauc, T.; Kamigaito, O. U.S. Pat. 4,739,007 (1988).
11. Kojima, Y.; Usuki, A.; Kawasumi, M.; Okada, A.; Fukushima, Y.; Kurauchi, T.; Kamigaito, O. J Mater Res 1992, 8, 1185.

12. Wu, T. M.; Chen, E. C.; Liao, C. S. Polym Eng Sci 2002, 42, 1141.
13. Wu, T. M.; Liao, C. S. Macromol Chem Phys 2000, 201, 2820.
14. Yeh, J. T.; Chang, C. J.; Tsai, F. C.; Chen, K. N.; Huang, K. S. Appl Clay Sci 2009, 45, 1.
15. VanderHart, D. L.; Asano, A.; Gilman, J. W. Chem Mater 2001, 13, 3796.
16. Yeh, J. T.; Xu, P.; Tsai, F. C. J Mater Sci 2007, 42, 6590.
17. Ellis, T. S. Polymer 2003, 44, 6443.
18. Liu, X.; Wu, Q. Polymer 2002, 43, 1933.
19. Pinnavaia, T. J.; Beall, G. W. Polymer–Clay Nanocomposites; Wiley: New York, 2000.
20. Finch, C. A. Polyvinyl Alcohol; Wiley: New York, 1992; Chapters 1–3 and 12–18.
21. Jang, J.; Lee, D. K. Polymer 2003, 44, 8139.
22. Casey, J. P.; Manley, G. B. In Proceedings of 3rd International Biodegradable Symposium; Applied Science: London, 1978.
23. Ha, C. S.; Lee, W. K.; Roe, T. W. Poly Bull 1993, 31, 359.
24. Lincoln, D. M.; Vaia, R. A.; Wang, Z. G.; Hsiao, B. S. Polymer 2001, 42, 1621.
25. Konishi, Y.; Cakmak, M. Polymer 2005, 46, 4811.
26. Jiang, T.; Wang, Y. H.; Yeh, J. T.; Fan, Z. Q. Eur Polym J 2005, 41, 459.